Sensor fusion-based precise obstacle localisation for automatic parking systems

J.K. Suhr and H.G. Jung✉

A precise obstacle localisation method for automatic parking systems is proposed. The proposed method improves the obstacle localisation accuracy by fusing only the sensors already installed on mass-produced vehicles. This method finds the initial obstacle location using ultrasonic sensors. On the basis of the initial obstacle location, it detects the obstacle's vertical outlines using images provided by an around view monitor system while the ego-vehicle is moving. The sequentially detected vertical outlines are combined based on the ego-vehicle positions estimated by built-in motion sensors. Finally, the obstacle location is refined by calculating the intersection point of the combined vertical outlines. In experiments, the proposed method was quantitatively evaluated and outperformed the previous method.

Introduction: As the demand for automatic parking systems increases, various parking space detection methods have been suggested [1]. Among them, the most widely used method in mass-produced vehicles is undoubtedly the ultrasonic sensor-based one. This method has been adopted by most car manufacturers. It typically finds vacant parking spaces using two ultrasonic sensors mounted on both sides of the front bumper [2]. Although ultrasonic sensors are inexpensive and easy to install, they have difficulties in finding narrow parking spaces due to low obstacle localisation accuracy. Light detection and ranging (LIDAR)-based [3] and motion stereo-based [4] methods can be used to enhance the obstacle localisation accuracy, but it is still difficult to apply them to mass-produced vehicles due to the sensor price or computation cost.

To overcome this problem, this Letter proposes a practical obstacle localisation method that utilises only the sensors already installed on mass-produced vehicles and a combination of simple algorithms. The proposed method fuses images produced by an around view monitor (AVM) system, range data given by ultrasonic sensors, and vehicle odometry obtained by built-in wheel speed and yaw rate sensors. Fig. 1 shows the sensor configuration. Red triangles and green dots indicate the four cameras of the AVM system and the two ultrasonic sensors, respectively, and the motion sensors are located inside the vehicle. The proposed method consists of three stages. First, it finds the initial obstacle location using the range data, which is obtained by registering the ultrasonic sensor outputs based on the vehicle odometry. Secondly, based on the initial obstacle location, it detects the obstacle's vertical outlines in images provided by the AVM system while the ego-vehicle is moving. The sequentially detected vertical outlines are combined based on the vehicle odometry. Finally, it precisely estimates the obstacle location by calculating the intersection point of the combined vertical outlines using the random sample consensus (RANSAC).

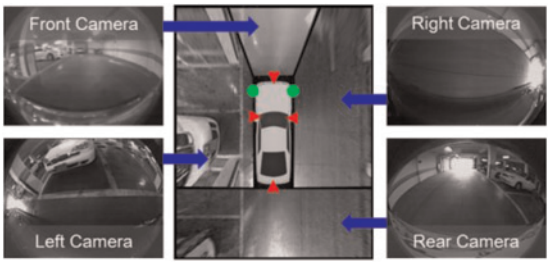

Fig. 1 *Sensor configuration: red triangles and green dots are four cameras of AVM system and two ultrasonic sensors, respectively*

Principle of the proposed method: This Letter deals with obstacles standing nearly perpendicular to the ground. Vehicles and pillars, which most frequently appear during parking, satisfy this condition. An AVM image is a combination of four bird's-eye view images, which are generated by virtually forcing the camera's optical axis perpendicular to the ground. Thus, in an AVM image, the vertical outline of the obstacle standing perpendicular to the ground is captured as a straight line segment whose extension passes through the camera location. This is because a straight line parallel to the camera's optical axis is captured as a straight line that passes through the image's principal point. The camera location is the principal point in an AVM image. Fig. 2*a* shows the images of the obstacle's vertical outlines (solid lines) and their extensions (dotted lines). It can be noted that the extended straight lines pass through the camera locations (triangles). In the rest of this Letter, we will refer to the straight line produced by extending the image of the obstacle's vertical outline as a vertical outline. In Fig. 2*a*, three vertical outlines are taken from the same parked vehicle while the ego-vehicle is moving. If these vertical outlines are registered based on the vehicle odometry, they form an intersection at the location, where the vertical outlines meet the ground as shown in Fig. 2*b*. Therefore, the exact location of the vertical outline can be calculated by estimating this intersection point.

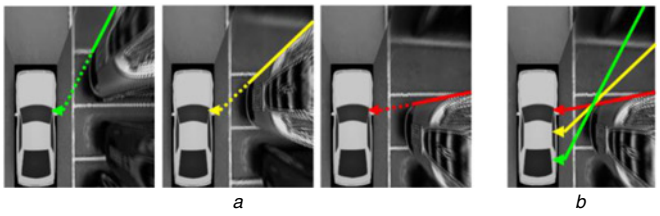

Fig. 2 *Principle of proposed method*
a Obstacle's vertical outlines captured in sequential AVM images
b Registered vertical outlines using vehicle odometry

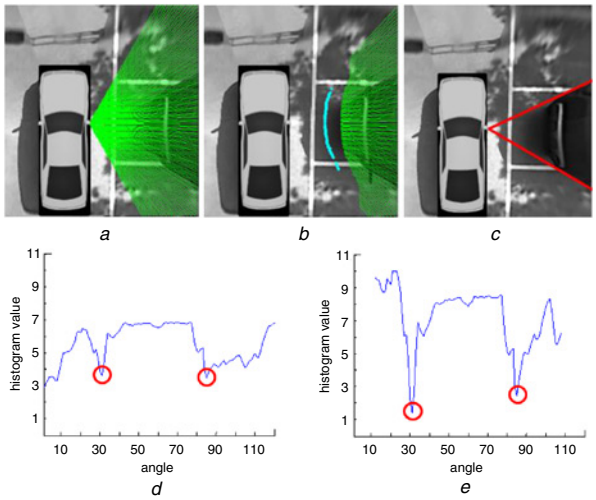

Fig. 3 *Polar histogram-based vertical outline detection*
a Initial radial lines
b Modified radial lines
c Detected vertical outlines
d Polar histogram generated by initial radial lines
e Polar histogram generated by modified radial lines

Vertical outline detection: Since the vertical outlines pass through the camera location, the proposed method detects them by generating a polar histogram from the camera location. The polar histogram is generated using a distance-transformed edge image instead of the original edge image in order to obtain a smooth histogram. When generating the polar histogram, it is important to exclude a non-obstacle area. In Fig. 3*a*, green lines show the radial lines used for generating the polar histogram. It can be seen that those radial lines include a large ground area, and this ground area will cause the polar histogram to have unclear valleys at the vertical outlines. Fig. 3*d* shows the polar histogram produced by the radial lines in Fig. 3*a*. It can be found that the valleys corresponding to the vertical outlines (red circles) are unclear. To reduce the effect of the non-obstacle area, the proposed method sets the starting points of the radial lines based on the range data, which is obtained by registering the ultrasonic sensor outputs using the vehicle odometry. In Fig. 3*b*, cyan dots and green lines show the range data and the modified radial lines, respectively. The modified radial lines include a less ground area than those in Fig. 3*a*. Fig. 3*e* shows the polar histogram generated by the modified radial lines in Fig. 3*b*. It can be noted that the valleys corresponding to the vertical outlines (red circles) are much clearer than those in Fig. 3*d*. In Fig. 3*c*, two red lines indicate the vertical outlines found from the modified polar histogram by detecting local minima lower than a predetermined value. The proposed method continuously

detects the vertical outlines while the ego-vehicle is moving, and the vertical outlines detected at different ego-vehicle locations are registered by the vehicle odometry.

Intersection point calculation: The obstacle location is refined by calculating the intersection point of the registered vertical outlines. An intersection point of multiple straight lines can be defined as a point that minimises the sum of the squared distances from multiple straight lines. The distance (d) between a point $\boldsymbol{x}$ and a straight line passing through a point $\boldsymbol{p}$ with a unit normal vector $\boldsymbol{n}$ can be calculated as

$$d = \left|(\boldsymbol{x}-\boldsymbol{p})^{\mathrm{T}}\boldsymbol{n}\right| \tag{1}$$

When there are N straight lines, the sum of the squared distances (e) can be calculated as

$$e = \sum_{i=1}^{N}(\boldsymbol{x}-\boldsymbol{p}_i)^{\mathrm{T}}(\boldsymbol{n}_i\boldsymbol{n}_i^{\mathrm{T}})(\boldsymbol{x}-\boldsymbol{p}_i) \tag{2}$$

By differentiating (2) with respect to $\boldsymbol{x}$, the point $\boldsymbol{x}'$ that minimises e can be obtained as

$$\boldsymbol{x}' = \left(\sum_{i=1}^{N}\boldsymbol{n}_i\boldsymbol{n}_i^{\mathrm{T}}\right)^{-1}\left(\sum_{i=1}^{N}\boldsymbol{n}_i\boldsymbol{n}_i^{\mathrm{T}}\boldsymbol{p}_i\right) \tag{3}$$

In real situations, the vertical outline detection procedure inevitably produces false positives, so-called outliers. These outliers severely hinder the aforementioned least-square-based estimation. Thus, the proposed method utilises the RANSAC [5] for a robust estimation. That is, two straight lines are randomly selected to calculate the intersection point, and then the straight lines close to the calculated intersection point are considered as its consensus set. This procedure is iterated and the intersection point that produces the largest consensus set is selected. Finally, the proposed method re-estimates the intersection point using all the straight lines included in the selected consensus set, so-called inliers using the least-square-based estimation. The final obstacle location is calculated by converting the location of the intersection point to the location of the real world using the camera parameters pre-calibrated during the AVM system installation.

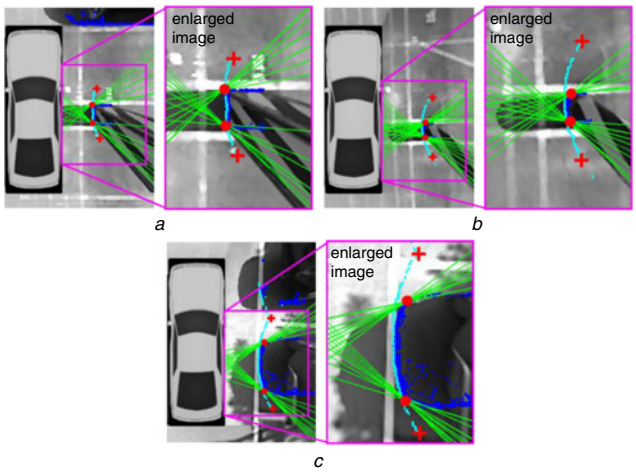

Fig. 4 *Obstacle localisation results of proposed method (red dots) and conventional ultrasonic sensor-based method (red crosses)*

a Rectangular pillar
b Circular pillar
c Parked vehicle

Experimental results: The proposed method was tested in 14 situations that include obstacles frequently presented in typical parking environments such as rectangular pillars, circular pillars, and parked vehicles. The test dataset was acquired by an AVM system, ultrasonic sensors, and built-in motion sensors installed on an off-the-shelf vehicle, Hyundai Azera. The performance of the proposed method was quantitatively evaluated and compared with the conventional ultrasonic sensor-based method [2]. To this end, the ground truth of the obstacle location was measured by a LIDAR. Figs. 4*a–c* show the obstacle localisation results of the proposed and conventional methods in cases of the rectangular pillar, circular pillar, and parked vehicle, respectively. In these figures, red dots and crosses indicate the obstacle locations estimated by the proposed and conventional methods, respectively. Cyan and blue dots are the range data given by the ultrasonic sensor and LIDAR, respectively, and green lines are the vertical outlines classified as inliers by the RANSAC. These figures show that the obstacle localisation results of the proposed method are more accurate than those of the conventional method. Note that it is important to estimate the precise locations of both ends of the obstacle in automatic parking systems.

Table 1 shows the obstacle localisation errors of the proposed and conventional methods. These errors were measured based on the ground truth obtained by the LIDAR. This table clearly shows that the obstacle localisation error of the proposed method (10.7 cm) is much lower than that of the conventional method (46.0 cm). The conventional method based on the ultrasonic sensor produces a large error in cases of rounded obstacles such as circular pillars and vehicle bumpers due to the lobe shape of the ultrasonic sensor. Since it provides different localisation errors depending on the obstacle shapes, its results cannot be corrected by a simple operation such as subtracting offset. The performance of the proposed method is degraded in the case of the vehicle bumper whose vertical outline is not perfectly perpendicular to the ground. However, the proposed method showed sufficient obstacle localisation accuracy in terms of the automatic parking systems.

Table 1: Comparison of obstacle localisation errors

Obstacle type	Proposed method (cm)	Conventional ultrasonic sensor-based method (cm)
Rectangular pillar	6.3	36.5
Circular pillar	9.3	67.4
Parked vehicle	16.7	44.5
Overall	10.7	46.0

Conclusion: The obstacle localisation error of the conventional ultrasonic sensor-based method cannot be corrected by an offset subtraction because its error depends on the obstacle shapes. To overcome this drawback, this Letter proposes a method that can accurately estimate obstacle locations by appropriately fusing the sensors already installed on mass-produced vehicles. The proposed method is expected to improve the performance of automatic parking systems, especially where the parking space is narrow or next to circular pillars.

Acknowledgment: This research was supported by the Hyundai Motor Company.

Submitted: *16 January 2018* E-first: *23 February 2018*
doi: 10.1049/el.2018.0196
One or more of the Figures in this Letter are available in colour online.

J.K. Suhr (*School of Intelligent Mechatronics Engineering, Sejong University, Seoul, Republic of Korea*)

H.G. Jung (*Department of Information and Communication Engineering, Korea National University of Transportation, Chungju, Republic of Korea*)

✉ E-mail: hogijung@ut.ac.kr

References

1 Lee, S., and Seo, S.-W.: 'Available parking slot recognition based on slot context analysis', *Intell. Transp. Syst.*, 2016, **10**, (9), pp. 594–604
2 Hyundai Advanced Driver Assistance System: 'Smart parking assist system'. Available at http://brand.hyundai.com/en/brand/technology/adas.do, accessed December 2017
3 Jung, H.G., Cho, Y.H., Yoon, P.J., *et al.*: 'Scanning laser radar-based target position designation for parking aid system', *Trans. Intell. Transp. Syst.*, 2008, **9**, (3), pp. 406–424
4 Unger, C., Wahl, E., and Ilic, S.: 'Parking assistance using dense motion stereo', *Mach. Vis. Appl.*, 2014, **25**, (3), pp. 561–581
5 Fischler, M., and Bolles, R.: 'Random sample consensus: a paradigm for model fitting with applications to image analysis and automated cartography', *Commun. ACM*, 1981, **24**, (6), pp. 381–395